Student thesis series INES nr 673

# Monitoring glacier mass change in northern Sweden from 2003 to 2023 using satellite altimetry data

Cheng Cheng

2024
Department of
Physical Geography and Ecosystem Science
Lund University
Sölvegatan 12
S-223 62 Lund
Sweden

**Cheng Cheng (2024).**
*Monitoring glacier mass change in northern Sweden from 2003 to 2023 using satellite altimetry data*
Master degree thesis, 30 credits in *GIS and Remote Sensing*
Department of Physical Geography and Ecosystem Science, Lund University

Level: Master of Science (MSc)

Course duration: *January* 2024 until *June* 2024

# Monitoring glacier mass change in northern Sweden from 2003 to 2023 using satellite altimetry data

---

Cheng Cheng

Master thesis, 30 credits, in *GIS and Remote Sensing*

Supervisor: Zheng Duan
Department of Physical Geography and Ecosystem Science, Lund University

Exam committee:
Micael Runnström, Department of Physical Geography and Ecosystem Science, Lund University
Babak Mohammadi, Department of Physical Geography and Ecosystem Science, Lund University

## Acknowledgement

First of all, I would like to express my gratitude to my thesis supervisor, Zheng Duan, for providing me with valuable ideas and guidance throughout the process of writing my master's thesis. He not only offered me insightful suggestions that greatly contributed to my research but also helped me navigate when I got frustrated, providing clarity on the overall direction of my study. Furthermore, I would like to extend my gratitude to Dr. Yubin Fan from Nanjing University for providing constructive comments that significantly improved this master's thesis.

Secondly, I would like to thank the Department of Physical Geography and Ecosystem Sciences at Lund University for offering high-quality courses that have provided me, a non-geography background student, with a comprehensive understanding of geography. Studying at Lund University marked my first time leaving my home country, and I spent considerable time adjusting to this new environment. I encountered moments of confusion and self-doubt, but ultimately, I overcame these challenges. That did not defeat me only served to make me stronger.

Thirdly, I would like to extend my gratitude to my classmates from the GIS and Remote Sensing Class of 2022. Coming from diverse backgrounds and corners of the globe, we shared two wonderful years together. During this time, we supported each other whenever we have trouble and often participated in social activities outside of class. I have gained valuable insights and formed genuine friendships in this incredibly diverse environment.

I also want to thank my parents, who despite being thousands of miles away in China, have always provided me with immense encouragement and support.

Lastly, I want to acknowledge my own efforts throughout this semester. While setbacks in research often left me feeling disappointed, the joy of finally achieving results made it all worthwhile.

## Abstract

The analysis of glacier mass changes in northern Sweden from 2003 to 2023 employed the non-repeat observation method, utilizing data from altimetry data ICESat and ICESat-2, along with Swedish national DEM and RGI v7.0 glacier boundary. The total volume decreased by -2.78 ± 0.58 $km^3$, corresponding to a total mass loss of 10.41 ± 6.60 m w.e. over the past two decades. These changes contribute approximately $6.52 \cdot 10^{-3}$ mm to global sea-level rise. The study reveals a general trend of glaciers losing mass throughout the observation period.

Additionally, in-situ measurements in northern Sweden were obtained to evaluate the results from the altimetry remote sensing method. The results are all reasonable compared to the in-situ measurements. Except for Storglaciären, the in-situ measurements of the other glaciers exhibit more negative mass balances compared to those measured by altimetry data. The relationship between glacier mass changes and temperature changes was also analyzed by comparing the average temperature during the glacier melt season with the annual average glacier mass balance obtained from the results. As the average temperature of melt season increases, the glacier mass changes increase.

Key words: Altimetry, Climate change, Glaciology, ICESat, ICESat-2, Mass change, Satellite, Sea-level rise, Sweden

## List of abbreviations

$B_n$: Net mass balance
$B_s$: Summer mass balance
$B_w$: Winter mass balance
DEM: Digital Elevation Model
GLIMS: Global Land Ice Measurements from Space
ICESat: Ice, Cloud, and land Elevation Satellite
ICESat-2: Ice, Cloud, and land Elevation Satellite-2
M w.e.: Meter water equivalent
NASA: National Aeronautics and Space Administration
RGI: Randolph Glacier Inventory
RMS: Root Mean Square
SMHI: Swedish Meteorological and Hydrological Institute
SRTM: Shuttle Radar Topography Mission

# Contents

## 1. Introduction

Global warming is a recognized global issue, with glacier changes serving as sensitive climate change indicators (Lemke et al., 2007). The rate of warming has accelerated significantly since 1980s (Allen et al., 2014). Glaciers worldwide show evident retreat, including reduced area, decreased mass, and rising boundaries (Paul et al., 2015). Glacier melt has significant implications for human societies. Notably, it contributes to global sea-level rise. Additionally, glacier melt influences local river runoff, thereby influencing nearby irrigation practices (Li et al., 2006). In regions renowned for their glaciers, tourism may experience a decline due to the disappearance of glaciers (Bowen, 2002).

Glacier mass balance is one of the most important features in estimating glacier change (Berthier et al., 2023). Traditionally, field observations have been the primary method for measuring glacier mass balance (Thibert et al., 2008). These in situ measurements are mainly based on pits, stakes, and cores. Researchers measure glacier melt by monitoring stakes ablation and snow accumulation from pits and cores in study areas (Berthier et al., 2023). Field measurements, however, can be very expensive due to the need for repeated manual measurements and are constrained by limited spatial coverage across glacier regions (Bamber et al., 2007). Modern remote sensing technology has revolutionized the study of glacier mass change by providing global coverage of remote sensing data at varying spatial and temporal resolutions (Paul et al., 2015).

There are three main satellite-based techniques for estimating glacier mass balance: geodetic DEM differencing (Hugonnet et al., 2021); satellite altimetry (Jakob et al., 2021); and satellite gravity (Yi et al., 2020). DEM differencing methods have been utilized to create maps of glacier elevation changes to estimate glacier mass changes. DEMs data are derived by using overlapping optical stereo-imagery or radar imagery (Berthier et al., 2023). Satellite altimetry including both radar and laser altimetry can measure the elevation changes of the Earth's surface. Regarding radar altimetry, data from CryoSat-2 satellite has been used widely since 2010. As to laser altimetry, data from three satellites: ICESat (2003-2009), ICESat-2 (2018-present), and GEDI (2018-present) has been generally employed. Similar to DEM differencing methods, the elevation changes here are converted to estimate glacier mass changes. Satellite gravity technique monitor glacier mass changes in a different way. By deploying two satellites in the same orbit but at different locations, variations in the Earth's mass influence each satellite differently, leading to changes in satellite direction and velocity. Distance changes are measured by both satellites using microwave ranging instruments. These small distance changes are then converted into estimations of glacier mass variations on Earth. Widely utilized in this methodology are satellite data from the GRACE (2002-2017) and GRACE-FO (2018- ) missions.

However, the analysis of glacier mass changes using the aforementioned methods is not without its challenges. Regarding the DEM differencing technique, inconsistencies may arise due to the use of different sources of satellite derived DEM data in different periods, complicating mass change studies (Paul et al., 2017). As to the laser altimetry method, there is data gap between ICESat and ICESat-2 mission causing missing data from 2010 to 2017. Although there is one Operation IceBridge mission operating from 2009 to 2019 to bridge the gap between two ICESat missions, the IceBridge mission does not cover northern Sweden region. This temporal discontinuity could present challenges for research encompassing this specific timeframe in Sweden. Regarding radar altimetry, signal scattering could cause elevation biases (Morris et al.,2022). Regarding satellite gravity technique, GRACE observations have a low spatial resolution of around 200 to 300 km, which could also pose some challenges especially where glaciers are small and scattered.

In Sweden, most glaciers are small and dispersed. The total glacier area in Sweden amounts to only 261.38 $km^2$, representing only 0.37% of the global glacier area. Although Swedish glaciers are less significant to the global mass changes compared to other regions, it has the potential to provide insights into regional climate variations (Belart et al., 2020). Due to the low spatial resolution, the satellite gravity technique is unsuitable for application in Sweden. Regarding the DEM differencing technique, there is a notable lack of high-quality optical stereo imagery in the study area. The available images are mostly obscured by thick cloud coverage. Consequently, satellite altimetry data (ICESat series) serves as the most reliable source for measuring glacier mass changes in Sweden. ICESat and ICESat-2 ground tracks also cover the entire northern Sweden.

Additionally, research on local glacier mass changes since the 21st century has mainly focused on the Tibetan Plateau area, Greenland, and the Antarctic region (Berthier et al., 2023; Zhao et al., 2022). Despite this, Northern Sweden remains a relatively understudied region since 2003, especially when compared with other European regions like Svalbard. The most recent studies on Swedish glacier mass changes have primarily focused on variations from 1910 to 2003 (Brugger et al., 2005). Bolin Centre For Climate Research at Stockholm University annually conducts in-situ measurements to estimate glacier mass changes in Northern Sweden. However, these in-situ measurements only cover limited glacier areas that represent only 6.21% of the whole glacier area in northern Sweden. The utilization of satellite data for estimating these changes holds significance, not only for encompassing areas beyond the coverage of in-situ measurements but also for facilitating comparisons with field estimations. Employing remote sensing technique to measure glacier change is also sustainable (Kääb, 2008).

This master's thesis aims to monitor glacier mass changes in northern Sweden from 2003 to 2023, addressing the gap in measuring Swedish glacier changes using altimetry data. The study will calculate total glacier mass changes, average annual mass balance, and their contributions to sea-level rise. The results will be compared with in-situ measurements conducted by the Bolin Centre for Climate Research. Additionally, the project will explore the relationship between glacier mass changes and climate variations in these regions. This study will also help assess the future impact of rising temperatures on glacier mass loss.

## 2. Background

### *2.1 Glacier mass balance*

Glacier mass balance refers to the change in the mass of a glacier over a specified period (Bamber & Payne, 2004). The unit for measuring glacier mass balance is the kilogram (kg). When the glacier mass balance is divided by the glacier area, it is referred to as the specific mass balance. This specific mass balance allows for direct comparisons between different glaciers across various years. The unit for specific mass balance is $\mathrm{kg} \cdot \mathrm{m}^{-2}$. which is often expressed as meter water equivalent (m w.e.). Water equivalent indicates the volume of water that would result from melting the snow or ice. The relationship between meter ware equivalent and $\mathrm{kg} \cdot \mathrm{m}^{-2}$ is shown in equation (1):

$$1\, m\, w.e. = \frac{1000 kg \cdot m^{-2}}{\rho_w} \tag{1}$$

where $\rho_w$ represents the density of water.

### *2.2 Laser Altimetry*

Laser altimetry constitutes a category of active remote sensing techniques (Florinsky, 2016). This method employs a specialized instrument known as a laser altimeter, which can be mounted on either a satellite, an aircraft, or a helicopter. The laser altimeter emits laser light directed towards the land surface. Upon interaction with the surface, a portion of this laser light is reflected back toward the altimeter, where it is detected. By analysing the total travel time of the laser light, the altimeter can estimate the distance between the land surface and the altimeter. This distance, denoted as the range (R), can be determined using the equation:

$$R = \frac{1}{2} \cdot c \cdot t = \frac{1}{2} \cdot D \tag{2}$$

where $c$ represents the speed of light, and $t$ denotes the total travel time of the laser light.

In Equation (2), the total distance travelled by the laser light (D) is twice the real distance (Range, R) between the land surface and the altimeter. Given the precise satellite orbit, it is possible to calculate the satellite's altitude relative to the global ellipsoid. Thus, the elevation of the laser footprint on the land surface can be determined by the difference in satellite altitude and the range between the altimeter and the land surface (Fig. 2.1).

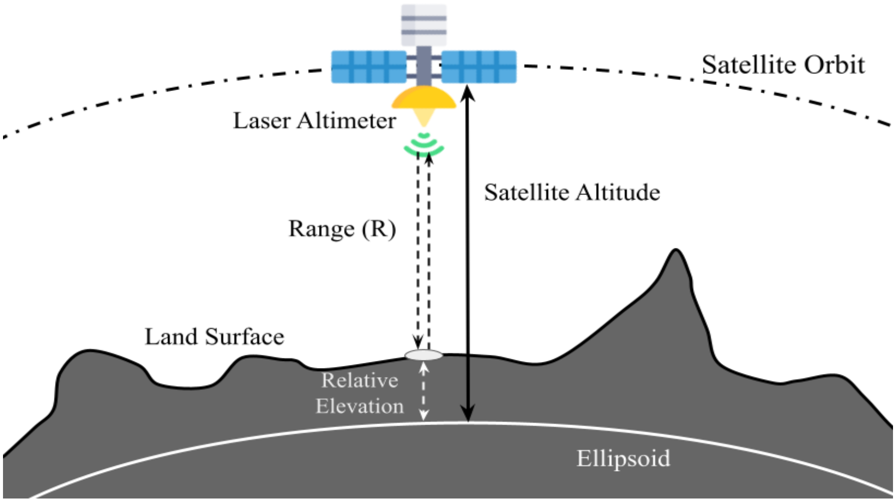

Fig. 2.1 A satellite laser altimeter measures the distance (Range, R) between it and the land surface by recording the travel time of laser light.

In addition to elevation, it is important to determine the geographical coordinates of footprints on the land surface. This is achieved with the aid of GPS receivers and navigation systems onboard the satellite. These systems enable the measurement of satellite location and orientation information, facilitating the determination of elevation geolocated to footprints on the land surface.

There are three primary forms of laser altimetry: satellite laser altimetry, aerial laser altimetry, and terrestrial laser altimetry (Florinsky, 2016). Satellite laser altimetry typically encompasses larger geographical areas globally, whereas aerial and terrestrial laser altimetry offer higher spatial resolution within specific regions. This master's thesis study mainly uses satellite laser altimetry to survey the entire northern Sweden region. Three Earth-orbiting satellite laser altimeter missions have been conducted: NASA's Ice, Cloud, and land Elevation Satellite (ICESat, 2003–2009), ICESat-2 (2018-present), and GEDI (2018-present). ICESat, ICESat-2 and their data platform OpenAltimetry will be discussed in subsequent sections (Table 1).

Table 1. Comparison between the characteristics of ICESat and ICESat-2. Characteristics includes number of beams, laser pulse frequency, wavelength, along track footprint distance and footprint size. (National Snow and Ice Data Center, 2024)

| Characteristics | ICESat | ICESat-2 |
| --- | --- | --- |
| Number of beams | 1 | 6 |
| Laser pulse frequency | 40 Hz | 10,000 Hz |
| Wavelength | 1064 nm | 532 nm |
| Along track footprint distance | 172 m | 0.7 m |
| Footprint size | 65 m | 11 m |

### *2.2.1 ICESat*

The ICESat (Ice, Cloud, and land Elevation Satellite) mission is aimed at measuring ice sheet mass balance, cloud and aerosol heights, as well as land topography and vegetation characteristics (Jairo, 2016). The ICESat satellite was launched on January 12, 2003, and remained operational until February 2010 (National Snow and Ice Data Center, 2024). From 2003 to 2009, ICESat provided multi-year surface heights of ice masses, as well as heights within Earth's atmosphere. The frequency of the ICESat laser pulse is 40 Hz, meaning it emits laser pulses 40 times per second, resulting in 172 m along-track spacing between pulses. The diameter of each ICESat footprint on the ground is approximately 65 meters (Schutz et al., 2005). ICESat data products include level-1 and level-2 products. For this master's thesis, the GLAH06 Level 1-B data is utilized. GLAH06 product records altimetry and Level 1-B data are data that have been processed to sensor units (National Snow and Ice Data Center, 2021). GLAH06 product is suitable for analysis in the study.

### *2.2.2 ICESat-2*

The ICESat-2 (Ice, Cloud, and land Elevation Satellite-2) is NASA's third mission in observing Earth's polar regions. Preceded by the ICESat mission (2003-2009) and Operation IceBridge mission (2009-2019), ICESat-2 was launched on September 15, 2018, and remains operational to date (National Snow and Ice Data Center, 2024). ICESat-2 employs 10,000 Hz pulse laser, enabling the emission of 10,000 pulses per second and resulting in 0.7 m along-track spacing between pulses. This rapid pulse laser technology significantly increases the number of footprints on the land surface compared to ICESat (Neumann et al., 2019). The laser pulse emitted by ICESat-2 is divided into three beam pairs, with each pair consisting of two beams. These beam pairs are spaced apart on the land surface by 3300 meters, and each individual beam within a pair is separated by 90 meters (Berthier et al., 2023). The footprint size is around 11m in diameter on ground (Luthcke et al., 2021). With a total of six beams, ICESat-2 can cover a significantly larger area along its satellite track compared to ICESat, which only utilized a single beam (Fig 2.2). ICESat-2 data products include level-1, level-2, and level-3 products. Among these, level-3 data "ATL06, Land Ice Height" and "ATL11, Land Ice Height Time Series" are the most suitable for measuring glacier mass changes (Kääb, 2008). For this master's thesis, the ATL06 product is utilized.

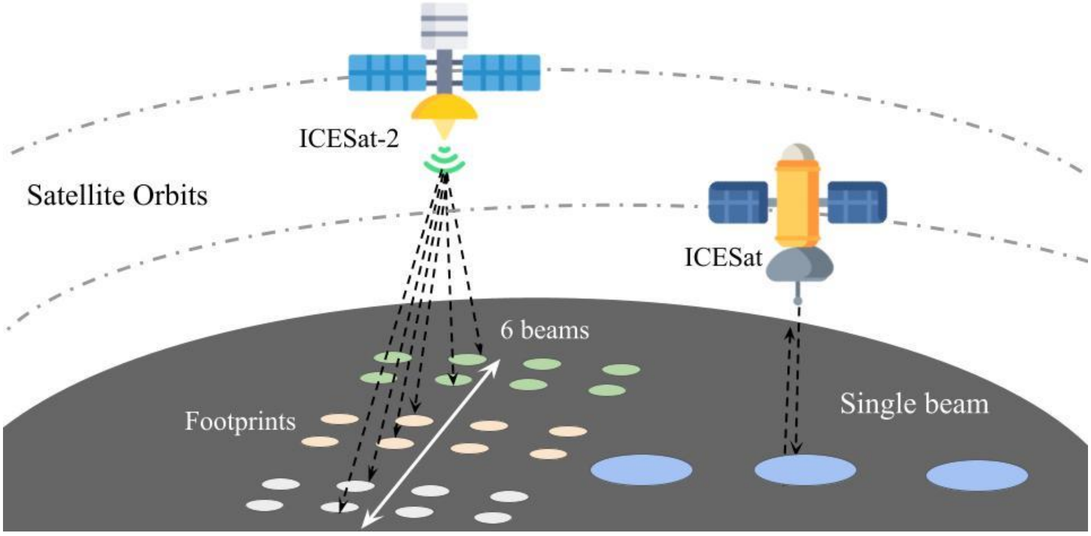

Fig. 2.2 Comparison between ICESat-2 and ICESat. (ICESat only emits one beam wile ICESat-2 emits 6 beams in total. ICESat footprints are 65 m in diameter and ICESat-2 footprints are only 11m in diameter. ICESat-2 has a very close along track footprint distance of 0.7 m, the distance of ICESat footprints is 172 m.)

### *2.2.3 OpenAltimetry*

OpenAltimetry is a web platform supported by NASA that allows users to discover and download data from both ICESat and ICESat-2 missions. It provides access to the GLAH06 data product from ICESat and seven altimetry data products including "ATL06, Land Ice Height" from ICESat-2 (National Snow and Ice Data Center, 2023). On OpenAltimetry, users can select and download data products with specific temporal and spatial information. Additionally, the platform visualizes footprints on the land surface along satellite orbits (Fig. 2.3). For this master's thesis, altimetry data is primarily obtained from this platform.

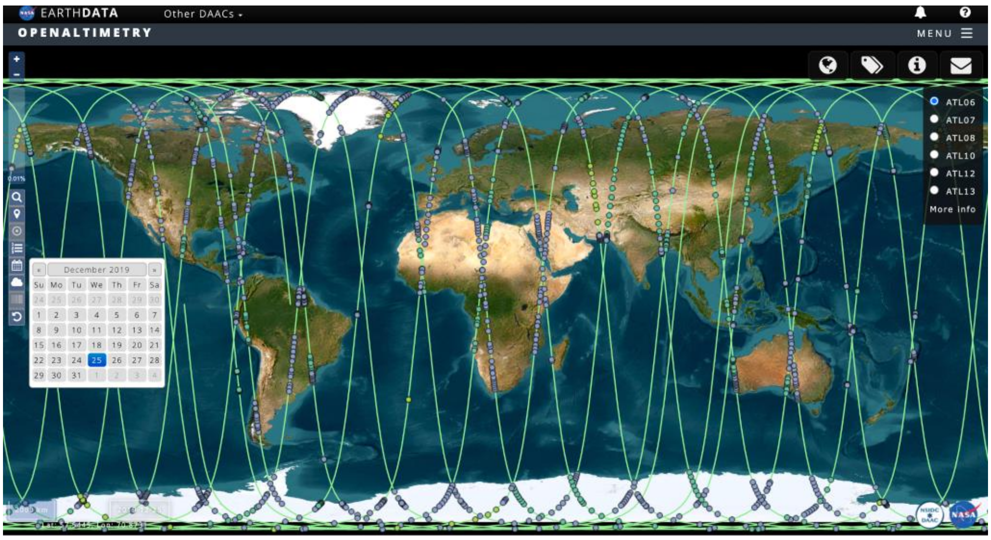

Fig 2.3 OpenAltimetry platform for ICESat-2 data. It shows the satellite orbit and footprints all over the world. (National Snow and Ice Data Center, 2023)

*2.2.4 Methods for estimating glacier changes using satellite altimetry*

Glacier changes are estimated by comparing altimetry data from the same locations at different time periods. Given the along-track spacing between footprints in both ICESat and ICESat-2 tracks, it is challenging to measure elevation differences at precisely the same locations. Variations in measurement locations can lead to significant elevation biases due to the inherent elevation differences across different locations. This elevation bias is referred to as "Slope error" (Berthier et al., 2021). "Slope error" poses even greater challenges in high mountain areas where steep terrain is common (Fig 2.4).

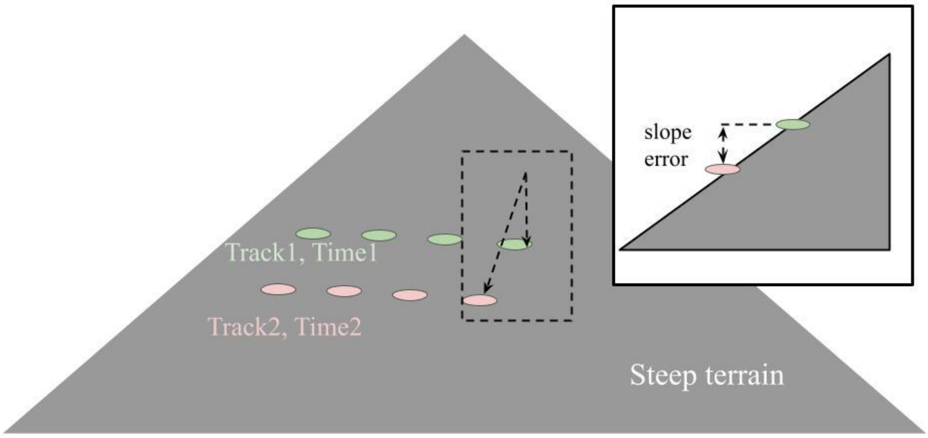


Fig 2.4 Slope error between track1 and track2 in steep terrain. Slope error exists between satellite track1 and track2.

There are two main methods for addressing the "slope error" caused by employing altimetry data. The first method involves calculating changes based on near-repeat observations, while the second utilizes non-repeat observations. For the near-repeat technique, some researchers calculate elevation differences at crossover points between two satellite footprint tracks (Brenner et al., 2007). Others use a reference DEM to correct for the slope error caused by two near-repeat tracks (Slobbe et al., 2008). Both methods require a sufficient number of near-repeat tracks and are most suitable for plain areas. However, in northern Sweden, ICESat tracks are quite sparse (Fig. 4.1). Additionally, the Swedish glacier area is among high mountains with steep terrain, which increases the potential for errors when employing near-repeat methods.

For non-repeat observation methods, a reference DEM is essential to calculate glacier changes. The reference DEM should be captured at a known date to avoid biases in elevation measurements. ICESat or ICESat-2 elevation measurements are then compared to this reference DEM to determine the relative elevation differences (Kääb, 2008). Glacier changes are estimated by comparing these relative differences over different time periods. However, this method may introduce additional uncertainties due to potential inaccuracies in the reference DEM.

For glacier change analysis, the SRTM (Shuttle Radar Topography Mission) DEM and its related products are commonly selected as reference DEMs, especially in the High Mountain Asia region (Fan et al., 2023). The SRTM measurements of Earth's elevation were conducted between February 11-22, 2000. This ensures that the DEM product has temporal consistency, making it ideal as a reference DEM. Unfortunately, the SRTM measurements only cover the ground from 57°S to 60°N. Since the glaciers in Sweden are mostly located between 67°N and 69°N, they fall outside the coverage range of the SRTM DEM. For this master’s thesis project, the Swedish national DEM, captured by aerial laser scanning, will be utilized as the reference DEM instead.

### *2.3 Glacier response to climate change*

Several factors influence glacier changes. The annual net mass balance is primarily influenced by temperature during the glacier melt season (April to September) and precipitation during the winter season (Bamber & Payne, 2004). As temperatures rise, glaciers melt and lose mass. Conversely, increased precipitation, especially in winter, results in greater mass accumulation on glaciers. These mass changes subsequently influence glacier geometry, leading to changes in both glacier area and glacier length. The rate at which glacier geometry responds to mass changes is referred to as the "response time" (Haeberli, 1995). The slope and size of the glacier also affect the response time; smaller glaciers with steep terrain respond more rapidly, leading to quicker advances or retreats (Jóhannesson et al., 1989). In this master's thesis, the focus is mainly on glacier mass changes, average height changes and their relationship with climatic variables. Further geometry and area changes of glaciers are not included in the scope of the study.

### *2.4 In-situ measurements in Sweden*

In-situ measurements of glaciers in northern Sweden have been conducted since 1946 (Holmlund & Jansson, 1999). The monitoring of Storglaciären represents the longest continuous record of distributed mass balance measurements in the world (Werner et al., 2024). These in-situ measurements include the determination of winter mass balance $B_w$ and summer mass balance $B_s$.

Winter balance is measured using fixed probing points and a varying number of snow density pits distributed across the glaciers. Summer balance, on the other hand, is assessed by placing stakes across the glaciers (Holmlund & Jansson, 1999). Typically, glaciers experience more ablation during the summer and more accumulation during the winter. The measurement of summer and winter balance is conducted at the beginning and the end of the glacier melt season, specifically in May and September. The annual net mass balance is calculated by summing the summer balance and the winter balance.

$$B_n = B_s + B_w \tag{3}$$

However, in-situ measurements in Sweden are confined to a limited number of glaciers, encompassing only 6.21% of the total glacier area in the country. This limitation underscores the importance of utilizing remote sensing techniques to gain a comprehensive understanding of glacier mass changes across the whole northern Sweden region.

In-situ measurement data is stored in Bolin centre for climate research at Stockholm University (https://bolin.su.se/data/tarfala/glaciers.php).

## 3. Study area

The total glacier area in Sweden is 261.38 km² (RGI Consortium, 2017), situated on the eastern side of the Scandinavian Mountain Range. The climate in this region is influenced by the North Atlantic Oscillation, but it tends to be more continental compared to the western side of the mountain range (Werner et al., 2024). Detailed climate data for this region are recorded at the Tarfala Research Station (67.91°N, 18.61°E).

For this study, glaciers without sufficient altimetry and valid DEM data are excluded, resulting in a study area that covers 86.67% of all Swedish glaciers. The geographical extent of this study area spans from 67°N to 68°30'N latitude and 17°E to 19°E longitude. This area is further segmented into three distinct regions: A, B, and C (Fig 3.1).

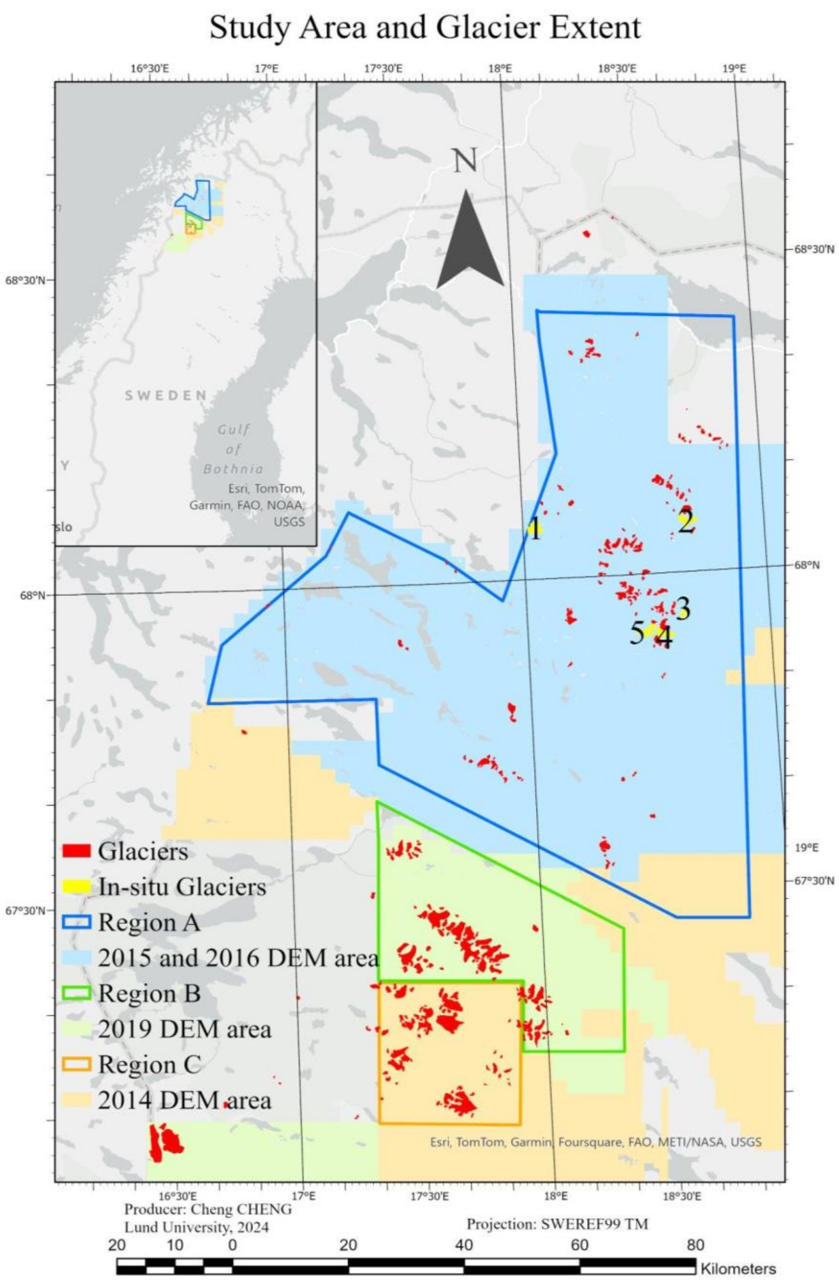

Fig 3.1 Study area and glacier extent in northern Sweden. Different colours indicate different study areas and their DEM data extent at different time.

The delineation of these regions is based on the acquisition periods of the reference DEMs, captured using aerial laser scanning. Specifically, the DEM in Region A was acquired from August 4, 2015, to October 5, 2015 and August 17, 2016, to October 7, 2016; the DEM in Region B was acquired from July 9, 2019, to September 22, 2019; and the DEM in Region C was acquired from July 8, 2014, to October 7, 2014 (Lantmäteriet, 2023). The reference DEMs in each region can be considered temporally consistent due to the relatively short acquisition periods.

In-situ glacier mass balance monitoring is conducted by the Bolin Centre for Climate Research at Stockholm University. The monitored glaciers are Mårmaglaciären (3.70 $km^2$, ID: 2), Rabots glaciär (3.69 $km^2$, ID: 5), Riukojietna (Total Area: 4.83 $km^2$, Area in Sweden: 4.09 $km^2$, ID: 1), Storglaciären (3.45 $km^2$, ID: 4), and Tarfalaglaciären (1.29 $km^2$, ID: 3) (Fig 3.2). All these glaciers are located within Region A.

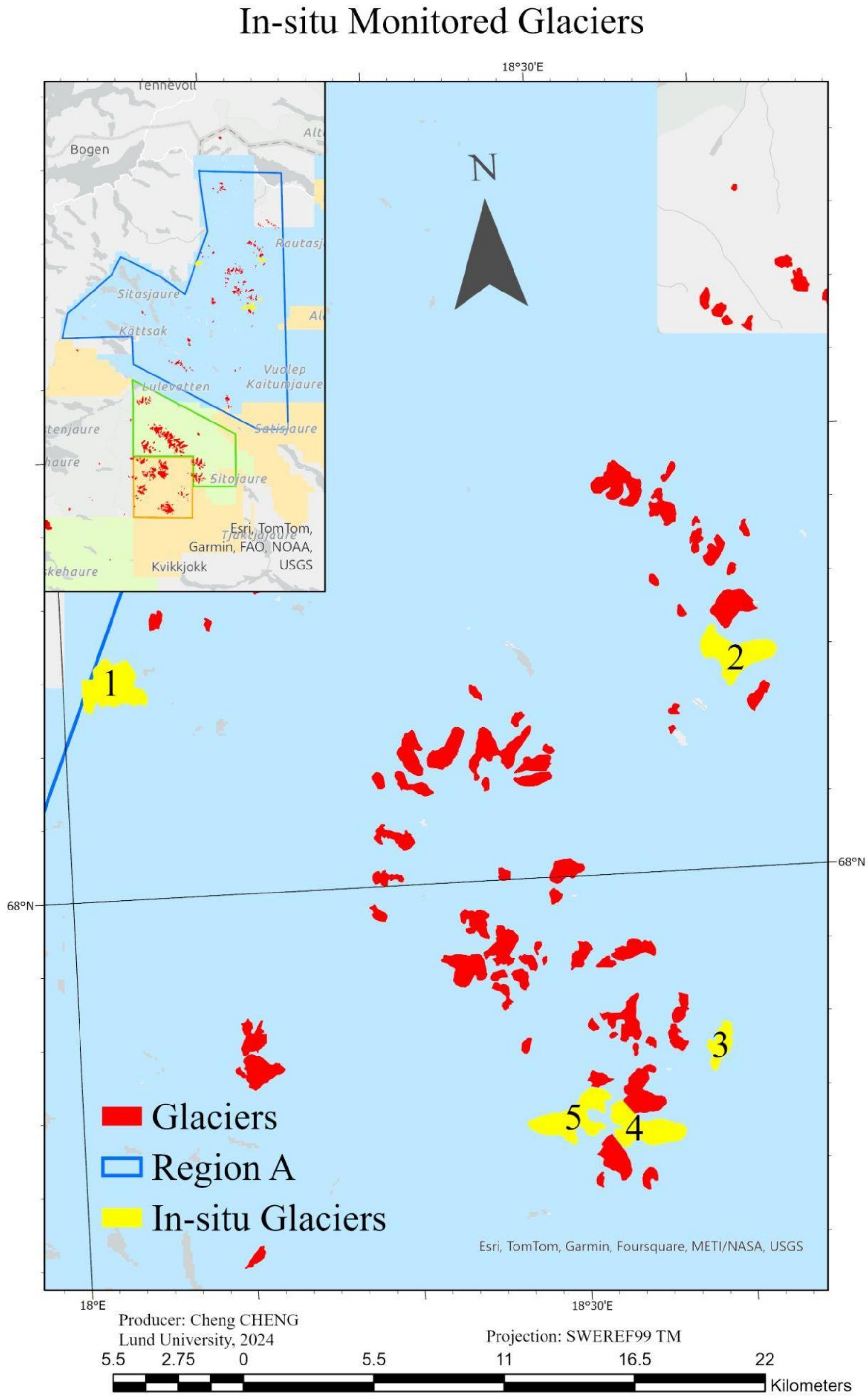


Fig 3.2 In-situ monitored glaciers with ID. The in-situ glaciers are Riukojietna (ID: 1) Mårmaglaciären (ID: 2), Tarfalaglaciären (ID: 3), Storglaciären (ID: 4) and Rabots glaciär (ID: 5).

# 4. Data sets

## *4.1 Altimetry data*

ICESat data from 2003 to 2009 in northern Sweden were retrieved from the OpenAltimetry platform. Due to the relatively small size of the study glacier area, there is a low probability of ICESat ground tracks intersecting with glacier extents (Fig 4.1). However, during Autumn (late August to late November), there tends to be a higher concentration of ICESat footprints within glacier extents compared to other seasons. Additionally, since the reference DEMs were all captured between July and October, comparing ICESat data and DEMs from the same season can help reduce errors. Therefore, for this project, footprints from Autumn were chosen for analysis.

ICESat-2 data from 2018 to 2023 were also obtained from the OpenAltimetry platform. With a total of six beams and a higher-frequency laser pulse, ICESat-2 data intersected much more with glacier extents than ICESat data (see Fig 4.2).

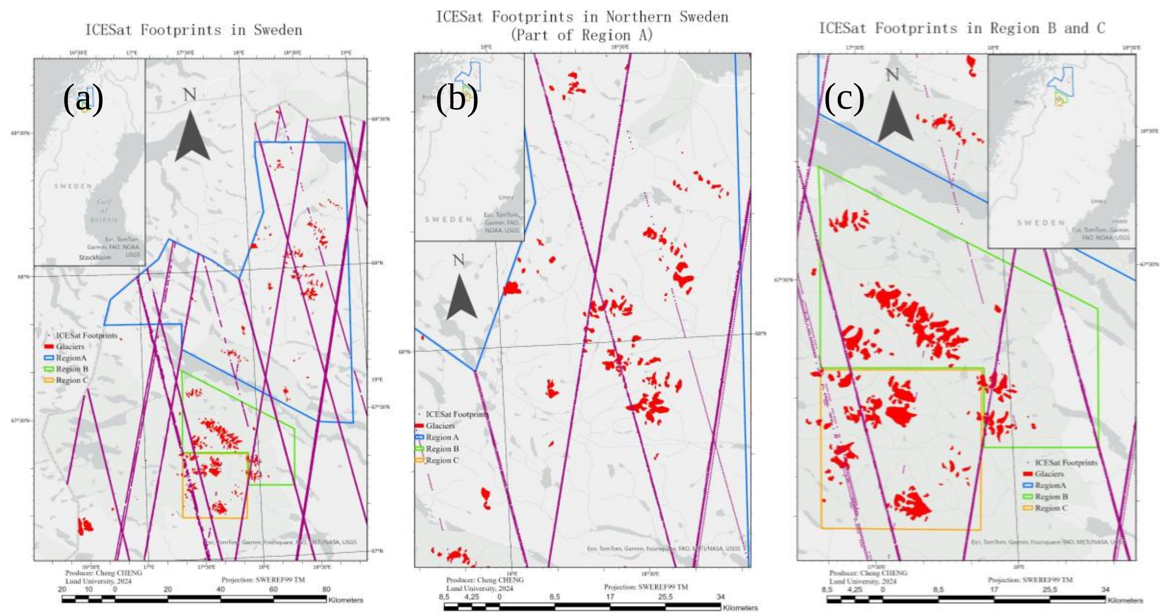


Fig 4.1 (a) ICESat footprints in Northern Sweden (b) Footprints in Part of Region A (c) Footprints in Region B and Region C

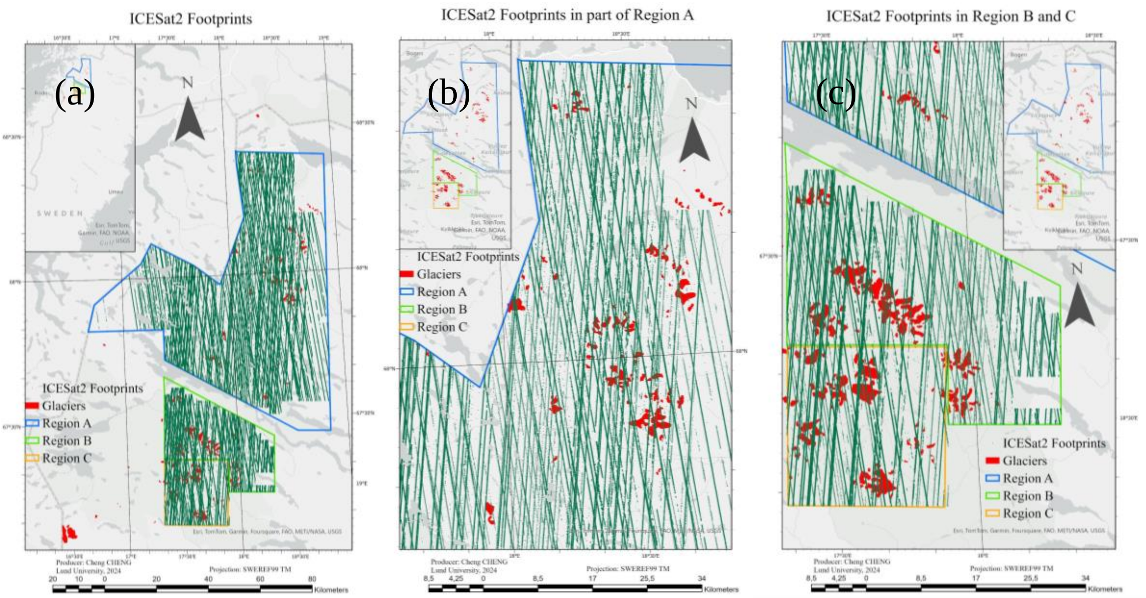


Fig 4.2 (a) ICESat2- footprints in northern Sweden (b) Footprints in Part of Region A (c) Footprints in Region B and Region C

## *4.2 Ancillary datasets*

### *4.2.1 Reference DEM*

Reference DEM data specific to the study area has been obtained from Lantmäteriet, generated in 2023. Lantmäteriet, an authority under the Swedish Ministry of Rural Affairs and Infrastructure, provided a product with a resolution of 50 meters based on the Sweden National Elevation Model. This terrain model is mainly produced through aerial image matching and laser data (Lantmäteriet, 2023). In the study area, all data is captured via aerial laser scanning. However, the time of laser scanning differs across the study area. Consequently, the area is divided into three regions based on the scanning period (Table 2).

Table 2. Time of laser scanning for reference DEM in different regions

| Region | Time of laser scanning |
|---|---|
| Region A | August 4, 2015 - October 5, 2015<br>&<br>August 17, 2016 - October 7, 2016 |
| Region B | July 9, 2019 - September 22, 2019 |
| Region C | July 8, 2014 - October 7, 2014 |

### *4.2.2 Glacier boundary dataset*

The glacier boundary dataset used in this study is sourced from the Randolph Glacier Inventory (RGI) version 7.0. The RGI is a globally comprehensive inventory of glacier outlines and is part of the database compiled by the Global Land Ice Measurements from Space (GLIMS) initiative. The RGI version 7.0, released on September 19, 2023, corrects a map projection shift problem affecting glaciers in northern Sweden near Kebnekaise that was present in version 6.0. The glacier boundary geometry and other information in the RGI dataset have been set to be as close to the year 2000 as possible. In RGI version 7.0, 58% of the glaciers are within a two-year interval around the year 2000, an improvement over the 48.9% in version 6.0 (RGI 7.0 Consortium, 2023).

For this master's thesis, ICESat and ICESat-2 footprints intersecting with the glacier boundaries will be selected to measure glacier mass changes. However, from 2003 to 2023, glacier boundaries may not remain stable, with geometry changes occurring in several glaciers. Fortunately, the impact of boundary changes due to these geometry variations will mostly be covered by the glacier boundary dataset set close to the year 2000. This is because the glaciers in northern Sweden are generally shrinking and glacier areas are mostly getting smaller.

Some Scandinavian glaciers cross the national border between Sweden and Norway. For this study, these glaciers are clipped to the Swedish extent, and mass changes will only be analysed on the Swedish side. For example, the entire area of the glacier Riukojietna, with ID: No.1 (Fig 3.2), is 4.83 km². However, only 4.09 km² of this glacier lies within the Swedish extent.

### *4.2.3 In-situ measurements*

In-situ measurements are sourced from the Bolin Centre For Climate Research at Stockholm University database. Although annual measurements are ongoing, the open data about glacier mass balance does not include the most up-to-date information (Table 3).

Table 3. Time of available glacier mass balance data in different in-situ glaciers and each in-situ glacier's area.

| Glacier | Area | Time of available glacier mass balance data |
|---|---|---|
| Riukojietna (ID:1) | 4.09 km² | 1986-2011 |
| Mårmaglaciären (ID:2) | 3.70 km² | 1990-2011 |
| Tarfalaglaciären (ID:3) | 1.29 km² | 1986-2011 |
| Rabots glacier (ID:4) | 3.45 km² | 1982-2011 |
| Storglaciären (ID:5) | 3.69 km² | 1946-2015 |

The annual data includes measurements such as winter mass balance, summer mass balance, net mass balance, equilibrium line altitude, and accumulation area ratio for each glacier (Moberg, 2011). Mass balance data is recorded in meter water equivalent units (m w.e.). For this master's thesis, in-situ measurements are used to evaluate the glacier mass change results obtained through remote sensing techniques.

### *4.2.4 Temperature data*

Temperature data for this region is recorded at the Tarfala Research Station (67.91°N, 18.61°E, 1143.65m). Climate records in Tarfala Valley have been maintained since 1946, and the first digital logger-based station was established at Tarfala in 1987 (Moberg, 2011). The Tarfala Research Station is centrally located in Region A (Fig 4.3). There are no research stations in Region B and Region C. Considering the variation in climate information in high mountain areas, data from surrounding research stations is not selected for analysis in Regions B and C. Relationship between glacier change and climate change is only analysed in Region A.

Climate data is obtained from the Swedish Meteorological and Hydrological Institute (SMHI). Unfortunately, precipitation data is only available from November 1, 1995, to November 1, 2000, at the Tarfala Research Station (SMHI, 2024). Therefore, for this master’s thesis, only monthly temperature data from 2003 to 2023 is used in the analysis.

Climate stations in study area

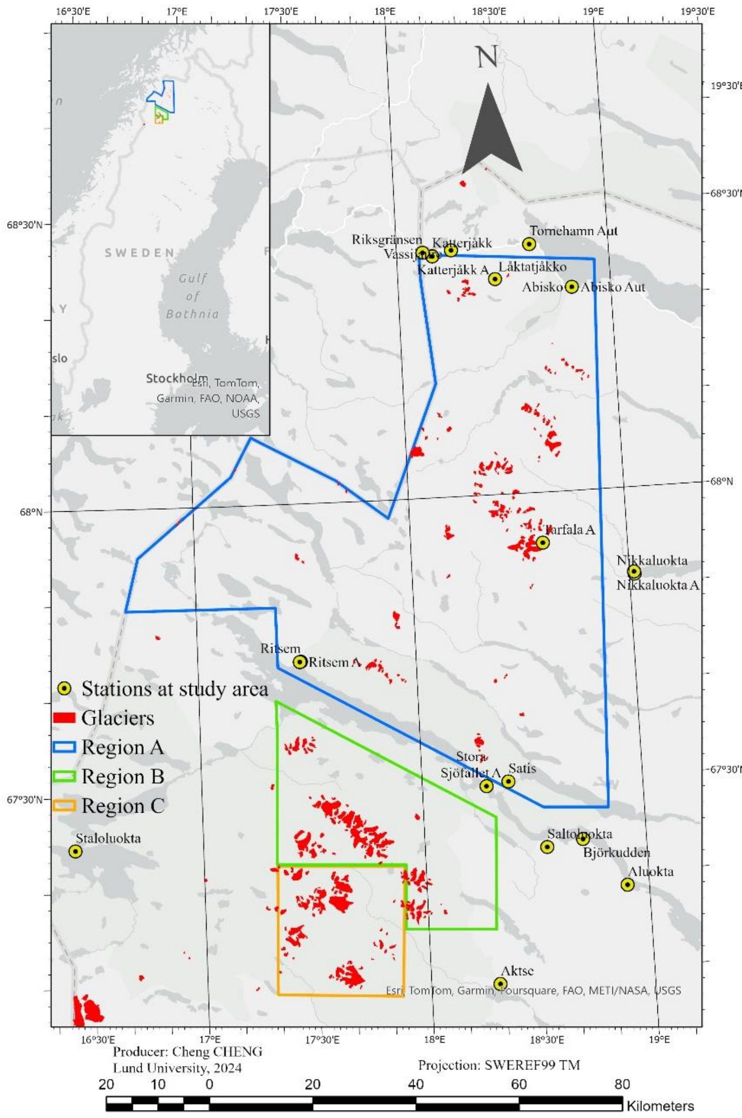


Fig 4.3 Climate Stations’ locations in and around each study area with the extent of glaciers

## 5. Methods

In northern Sweden, ICESat tracks are quite sparse, and the glaciers are situated in high mountains with steep terrain. This makes it unsuitable to employ the near-repeat observation method. Consequently, the non-repeat observation method was selected for further analysis. The workflow for this study is illustrated in Fig 5.1. Firstly, input data of certain season is selected. Secondly, co-registration is conducted to remove the elevation differences between different datasets. Thirdly, abnormal data is filtered out

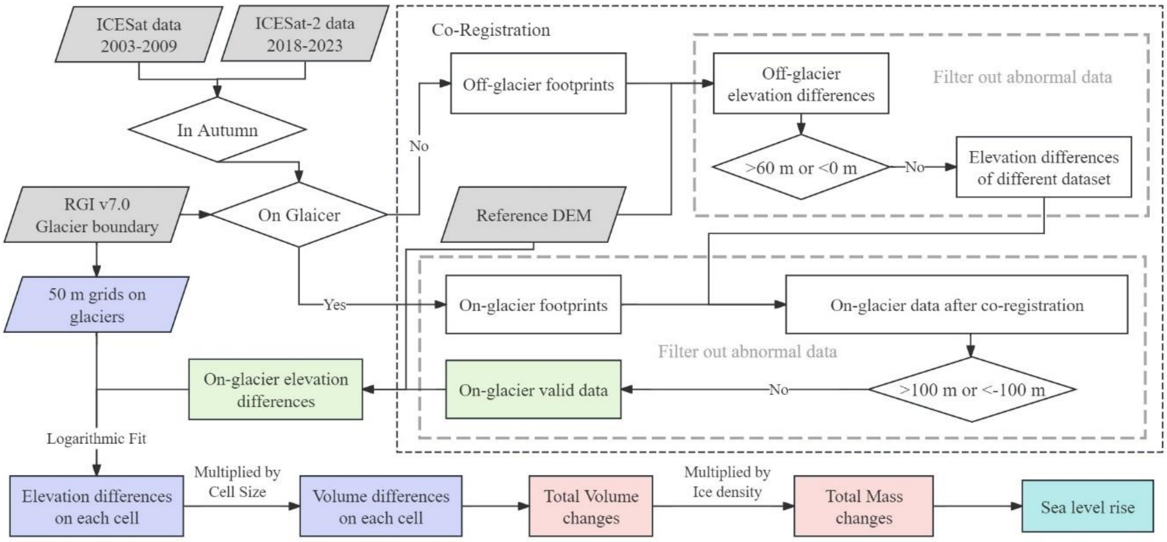


Fig 5.1 Workflow for measuring glacier mass changes from 2003 to 2023. The whole workflow includes co-registration of difference dataset, filtering out abnormal altimetry data and solving the problem of representativeness of the altimetry footprints.

ICESat data from 2003 to 2009 and ICESat-2 data from 2018 to 2023 were obtained. Considering that the reference DEM was captured between July and October, it is appropriate to use altimetry data also from the autumn season. Additionally, seasonal variations in snow thickness during summer and winter can introduce significant elevation errors, making it unsuitable to analyse glacier changes during these periods (Kääb, 2008). Therefore, ICESat and ICESat-2 data captured in autumn season (late August to late November) were selected for further analysis.

### *5.1 Co-registration of difference datasets*

There is an elevation difference between the reference DEM and altimetry data (Fig 5.2), making it necessary to perform co-registration of these datasets (Fan et al., 2023). Ideally, there should be no elevation change outside the glacier areas, implying no elevation difference between the reference DEM and altimetry footprints in these regions. The altimetry data footprints outside the glacier areas are referred to as off-glacier data.

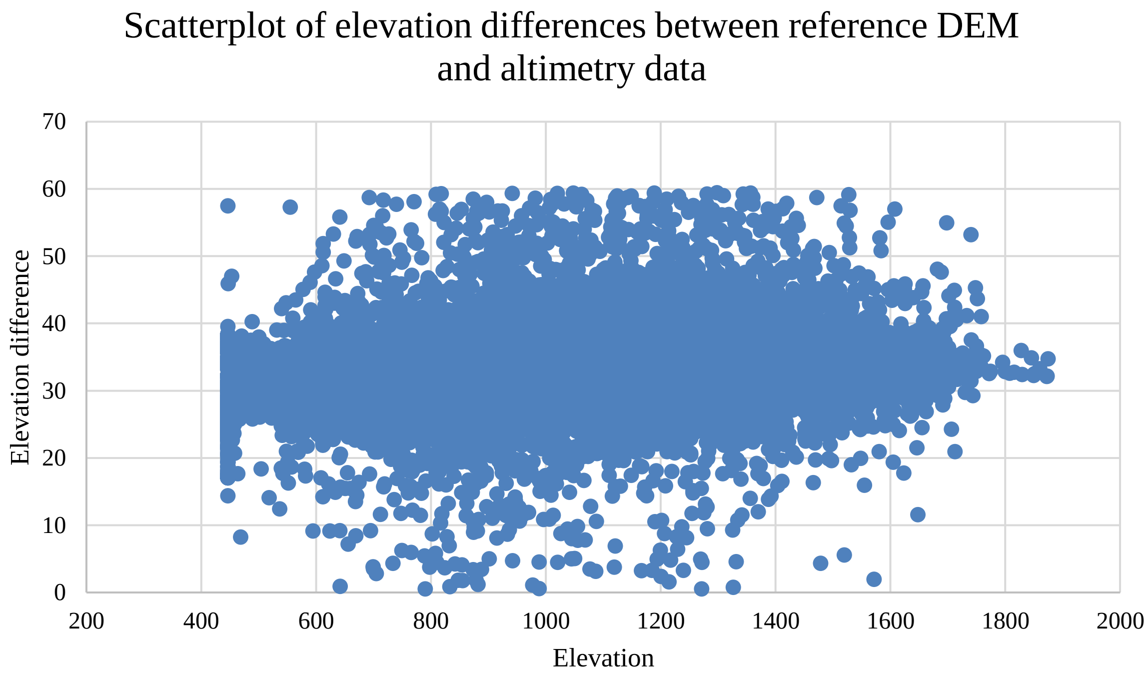


Fig 5.2 Scatterplot of elevation differences between reference DEM and altimetry data

It is common for some off-glacier footprints near the glacier boundary to experience elevation changes. Therefore, it is crucial that the off-glacier footprints selected for calculating elevation difference are not close to the glacier boundary. A 500-meter buffer is created outside the glacier boundary, and all footprints outside this buffer are considered valid off-glacier data. After filtering out abnormal off-glacier data (a process discussed in the next section), the elevation difference is calculated as the average elevation differences between the reference DEM and the off-glacier altimetry data. This elevation difference is then added to the on-glacier altimetry elevation data to complete the co-registration process. For this master's thesis, the elevation difference is approximately 32 meters.

### *5.2 Filter out abnormal altimetry data*

Cloud cover can introduce significant errors in altimetry data. As shown in Fig. 5.2, any footprint elevation exceeding 2200 meters is likely influenced by cloud cover, considering the highest peak in Sweden is only 2104 meters. For off-glacier footprints, any elevation difference between the altimetry data and the reference DEM greater than 60 meters or less than 0 meters is excluded. After co-registration, for on-glacier footprints, elevation differences exceeding 100 meters or less than -100 meters are removed to ensure accuracy (Kääb, 2008).

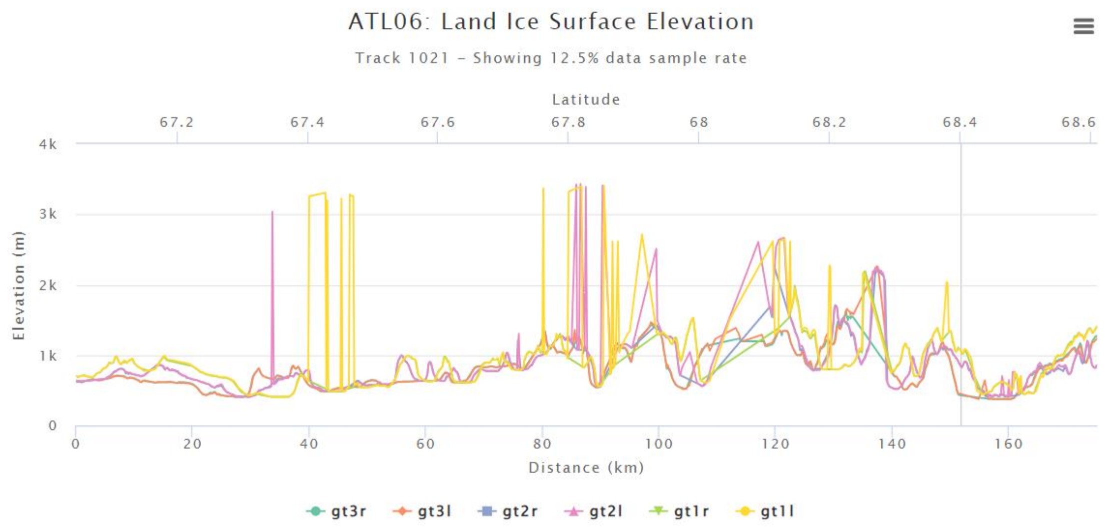


Fig 5.3 ICESat-2 footprints' elevation series and abnormal elevation data in ICESat-2 (National Snow and Ice Data Center, 2023)

### *5.3 Representativeness of the altimetry footprints*

Table 4. Number of ICESat and ICESat-2 satellite footprints on the glaciers

| Study Area | Number of ICESat footprints | Number of ICESat-2 footprints |
|---|---|---|
| Whole Area | 229 | 22327 |
| Region A | 92 | 5338 |
| Region B | 90 | 8034 |
| Region C | 47 | 8955 |

ICESat and ICESat-2 on-glacier footprints do not cover the entire glacier area in northern Sweden (Fig. 4.1, Fig. 4.2, Table 4). Directly calculating the average elevation differences may be unsuitable because the footprints do not represent the entire glacier area, such that an extrapolation to the entire glacier area is necessary. Researchers have found that there is a relationship between glacier elevation changes and the elevation itself on glaciers (Kääb, 2008). Typically, as elevation increases, elevation changes become smaller. This relationship is nonlinear. To accommodate this nonlinear relationship, logarithmic fit is applied in different study regions at different times to establish this relationship.

To apply this relationship to all glaciers in the study area, grids are created based on the glacier boundary. The grid size is set at 50m x 50m, matching the resolution of the reference DEM. An example of these grids on Storglaciären is shown in Fig. 5.3. For each cell in the grids, an elevation difference is calculated based on the elevation data at that cell. This method allows for the estimation of elevation changes across the entire glacier area. The glacier volume change for each cell is then calculated by multiplying the elevation difference by the cell size. The total volume change for the glacier is obtained by summing up the volume changes of all the cells.

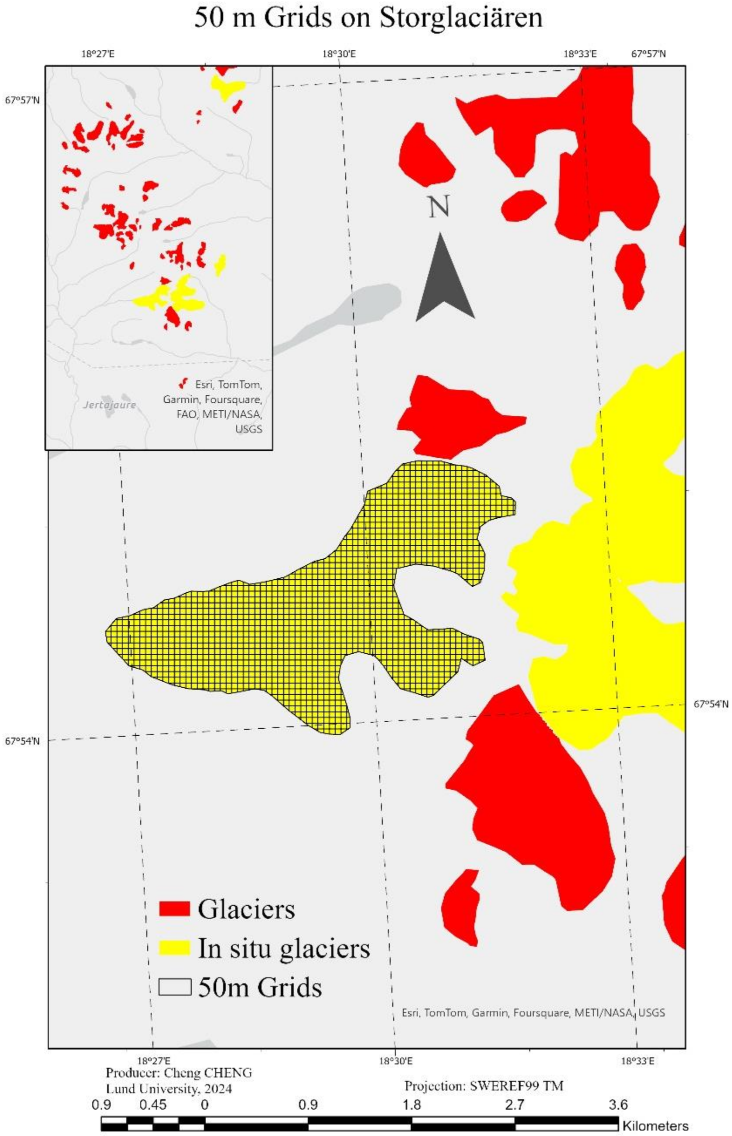


Fig 5.4 50m x 50m grids created on Storglaciären. Further computation is based on each cell inside the grids.

### *5.4 Mass changes and sea-level rise*

Volume change is converted to mass change by multiplying it by the glacier ice density. A glacier ice density of $850 \pm 60\ kg \cdot m^{-3}$ is used, as it is suitable for a wide range of conditions (Huss, 2013). This approach allows for the estimation of glacier mass changes across the entire study area.

Since all Swedish glaciers are above sea level, the mass loss from these glaciers will contribute to global sea level rise. The oceans globally cover an area of $3.618 \cdot 10^{8} km^{2}$. The global sea level rise contributed by the glaciers is obtained by dividing the total water volume loss by the global ocean area.

### *5.5 Mass balance uncertainty analysis*

Uncertainty in estimating mass balance in this master's thesis primarily originate from three sources: glacier area error ($\sigma_A$), elevation change error ($\sigma_h$), and glacier density error ($\sigma_{den}$). Elevation change error for every study area and year is estimated by equation (4) (Moholdt et al., 2010)：

$$\sigma_h = \frac{\sigma_{fit}}{\sqrt{N-2}} \tag{4}$$

where $\sigma_{fit}$ is the RMS error of the logarithmic fit, −2 is the degree of freedom, and N is the number of uncorrelated elevation change observations in the region. The degree of freedom is 2 since there are 2 unknown parameters in the logarithmic fit function. However, calculating elevation differences between 2003 and 2023 requires the use of the reference DEM, introducing double errors in this process. Therefore, the total elevation change errors should be:

$$\sigma_H = \sqrt{\sigma_{h1}^2 + \sigma_{h2}^2} \tag{5}$$

where $\sigma_{h1}$ represents the errors of the differences between ICESat data in 2003 and reference DEM, $\sigma_{h2}$ represents the errors of the differences between ICESat-2 data in 2023 and reference DEM.

Glacier volume uncertainties ($\sigma_V$) are affected by uncertainty in elevation difference ($\sigma_H$) and glacier area ($\sigma_A$):

$$\sigma_V = \sqrt{(\sigma_H \cdot A)^2 + (\sigma_A \cdot dH)^2} \tag{6}$$

where A represent the regional glacier area, dH represents the average elevation difference. Glacier area uncertainty $\sigma_A$ is $\pm 10\%$ (Berthier et al., 2010). Glacier mass uncertainties ($\sigma_M$) are influenced by the uncertainties in glacier volume ($\sigma_V$) and uncertainties in glacier density ($\sigma_{den}$) (Fan et al., 2023):

$$\sigma_M = \sqrt{(\sigma_V \cdot \frac{\rho_g}{\rho_w \cdot A})^2 + (\sigma_{den} \cdot \frac{V}{\rho_w \cdot A})^2} \tag{7}$$

where $\rho_g$ is the glacier density ($850 kg \cdot m^{-3}$), $\sigma_{den}$ is the uncertainties in glacier density ($\pm 60\ kg \cdot m^{-3}$). $\rho_w$ is the density of water ($1000 kg \cdot m^{-3}$).

## 6. Results

### *6.1 Glacier mass changes from 2003 to 2023*

From Table 5, the total glacier ice volume loss from 2003 to 2023 in the study area is 2.78 km³. This corresponds to a total water loss of 2.36 km³, which contributes approximately $6.52 \cdot 10^{-3} mm$ to global sea-level rise. Region B exhibits the largest mass changes and the lowest average annual mass balance over the two decades, whereas Region A has the lowest mass changes and the highest annual mass balance. However, Region A also has the largest mass change uncertainties. This may be due to the sparser spatial distribution of glaciers in Region A, which can introduce greater variability and errors in the measurements.

Table 5. Ice volume changes, mass changes and average annual mass balance in different areas from 2003 to 2023

| Study Area | Area (km²) | Ice volume changes (km³) | Mass changes ($m$ w.e.) | Average annual mass balance ($m\, y^{-1}$ w.e.) |
|---|---|---|---|---|
| Whole Area | 226.53 | -2.78 $\pm$ 0.58 | -10.41 $\pm$ 6.60 | -0.52 $\pm$ 0.33 |
| Region A | 77.92 | -0.83 $\pm$ 0.39 | -9.07 $\pm$ 4.29 | -0.45 $\pm$ 0.22 |
| Region B | 82.74 | -1.18 $\pm$ 0.33 | -12.07 $\pm$ 3.50 | -0.60 $\pm$ 0.17 |
| Region C | 65.87 | -0.77 $\pm$ 0.27 | -9.91 $\pm$ 3.60 | -0.50 $\pm$ 0.18 |

The map depicting the spatial variation of the average annual mass balance in Region A is shown in Fig. 6.1. There are noticeable variations both within a single glacier and between different glaciers. According to the extrapolation method used to create this map, glaciers at higher altitudes experience less mass loss compared to those at lower altitudes. This indicates that in this map, glaciers at higher elevations have a higher annual mass balance than those at lower elevations.

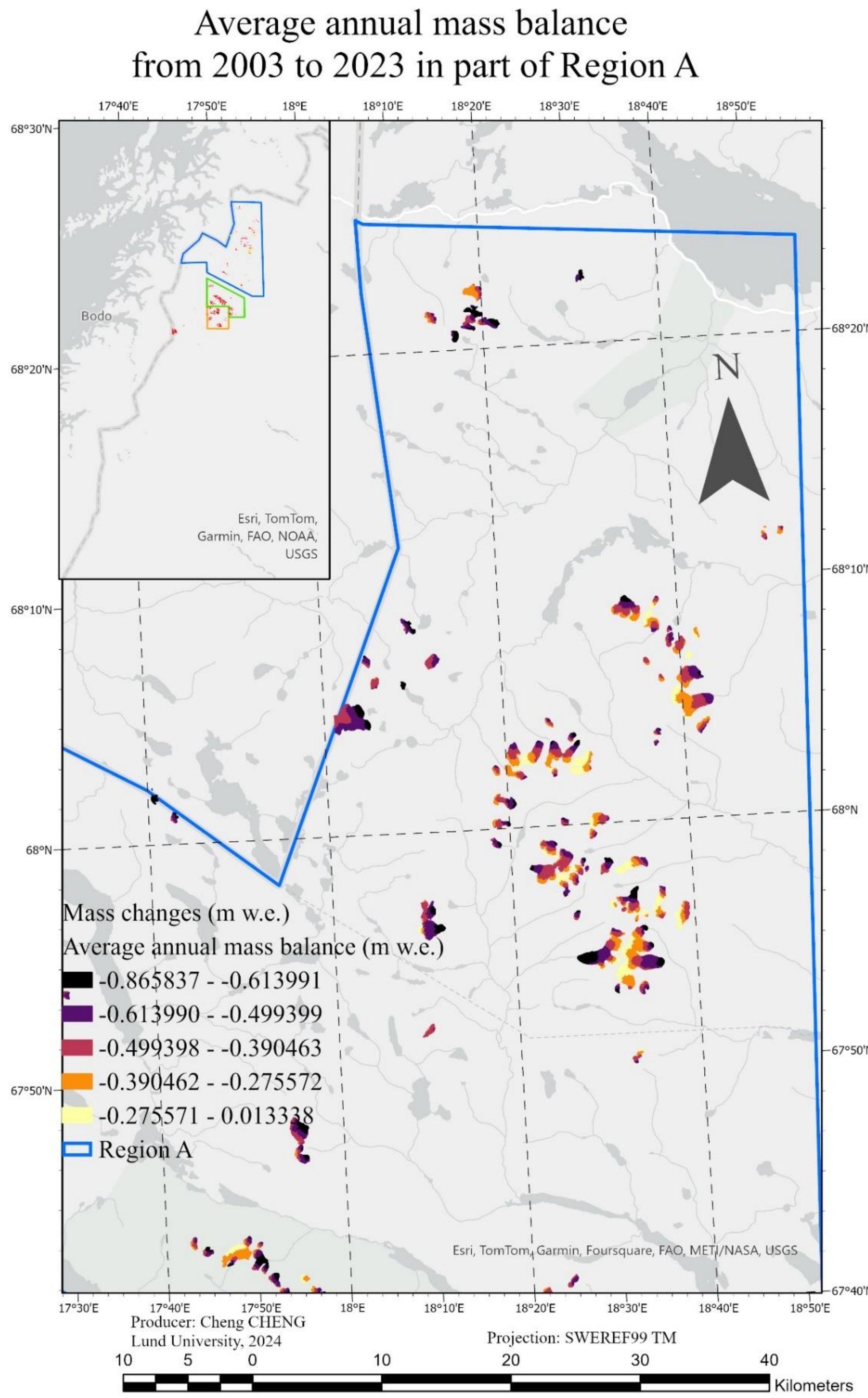


Fig 6.1 Average annual mass balance from 2003 to 2023 in part of Region A

The glacier mass change time series in Region A from 2003 to 2023 are presented in Fig. 6.2. It should be noted that the glacier mass changes are relative values, as they are all compared to the glacier state in 2003. Data from years 2003, 2005, 2006 and 2018 to 2023 is utilized. In the years 2004 and 2007 to 2009, there were no ICESat footprints on glaciers during the autumn season, and thus the glacier mass change results are not available for those years.

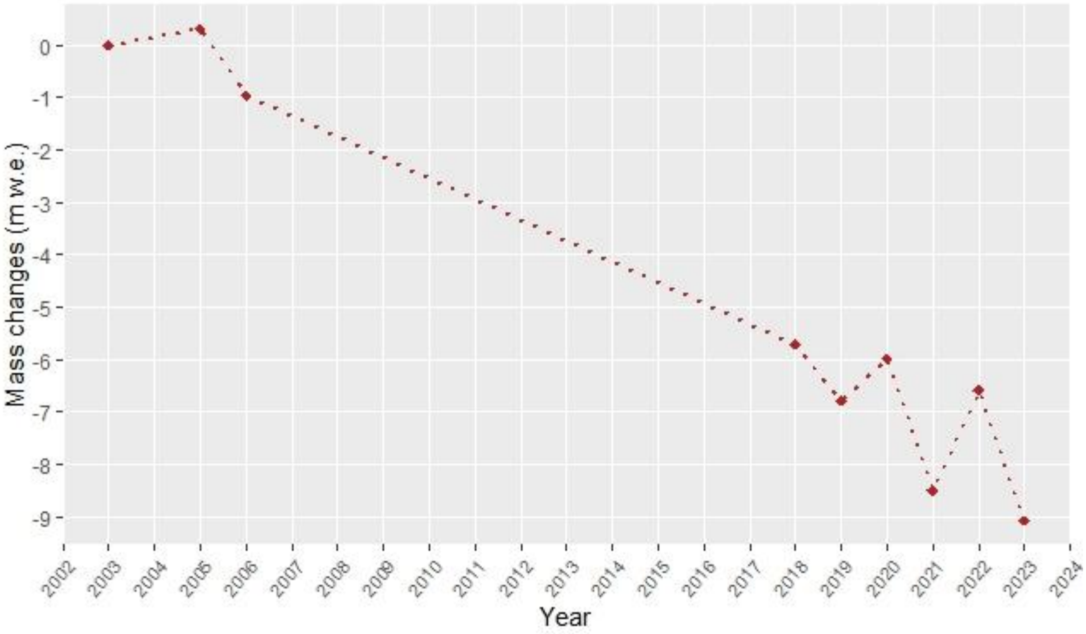


Fig 6.2 Glacier mass change time series in Region A from 2003 to 2023

From the time series figure, it is evident that glaciers are generally losing mass over the study period. However, in certain years, specifically 2005, 2020, and 2022, there is an observed increase in glacier mass compared to the previous year. This fluctuation is likely influenced by climatic factors. The relationship between glacier mass balance and climate variations will be thoroughly discussed in a later section.

### *6.2 Comparison with in-situ measurements*

In-situ measurements do not cover the entire two-decade period (2003-2023) due to limitations in open data availability. The available data, along with their respective time spans, are shown in Table 6. Except for Storglaciären, the in-situ measurements of the other glaciers exhibit more negative mass balances compared to those measured by altimetry data. This could be due to differences in the glacier boundaries used in these methods. Detailed analysis will be discussed in the discussion section.

Table 6. Comparison of mass balance with in-situ measurements in different area

| | | Average annual mass balance | |
|---|---|---|---|
| Study Area | Area | Measured by altimetry data (2003-2023) | In-situ measurement (with measured time span) |
| Riukojietna (ID:1) | 4.09 km² | -0.55 $\pm$ 0.27 $m\ y^{-1}$w.e. | -0.87 $m\ y^{-1}$w.e. (2004-2011) |
| Mårmaglaciären | 3.70 km² | -0.37 $\pm$ 0.27 $m\ y^{-1}$w.e. | -0.85 $m\ y^{-1}$w.e. |

| | | | |
|---|---|---|---|
| (ID:2) | | | (2003-2011) |
| Tarfalaglaciären (ID:3) | 1.29 km² | -0.33$\pm$ 0.27 $m\ y^{-1}$w.e. | -1.05 $m\ y^{-1}$w.e. (2003-2011) |
| Rabots glaciär (ID:4) | 3.45 km² | -0.44 $\pm$ 0.27 $m\ y^{-1}$w.e. | -1.03 $m\ y^{-1}$w.e. (2004-2006,2007-2011) |
| Storglaciären (ID:5) | 3.69 km² | -0.51 $\pm$ 0.27 $m\ y^{-1}$w.e. | -0.35 m w.e. (2003-2015) |

### *6.3 Relationship between annual mass balance and temperature data*

The annual mass balance of a glacier can be estimated by examining the changes in glacier mass over time. The mass balance of a glacier in a given year is simply the difference in mass between the previous year and the current year. The mass balance is primarily influenced by the temperature during the glacier melt season. The mass balance and average temperature during the melt season in Region A are presented in Fig. 6.3.

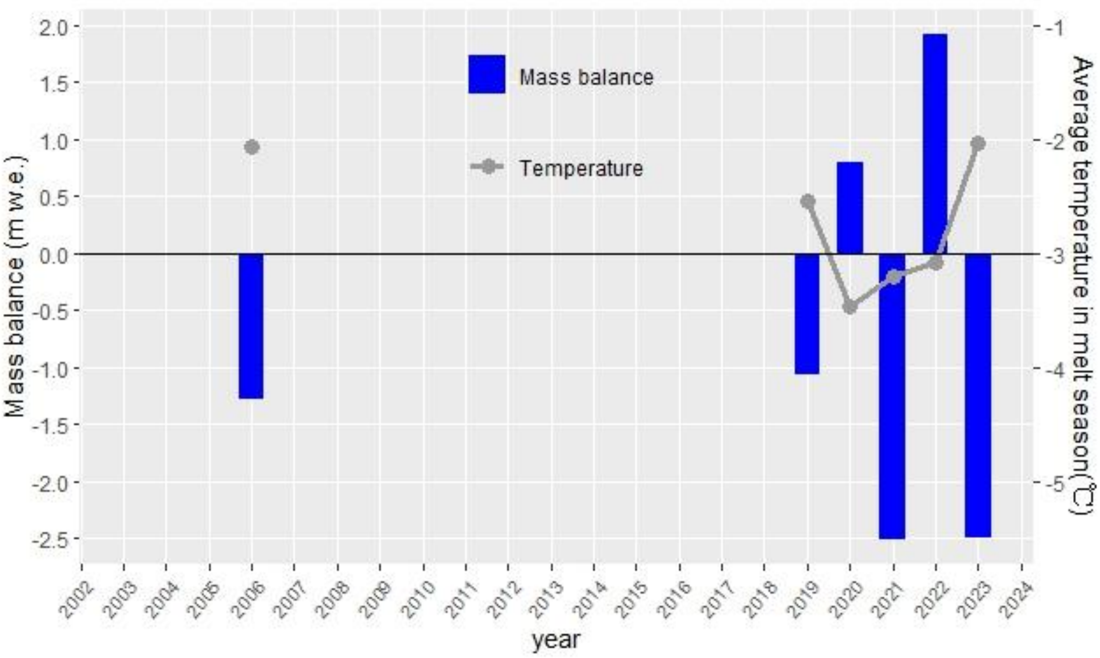


Fig 6.3 Mass balance and average temperature in glacier melt season of Region A

From the figure, when the mass balance is positive (e.g., in 2020 and 2022), the average temperature during the glacier melt season is consistently lower than -3 degrees Celsius. Conversely, when the mass balance is negative, except for the year 2021, the average temperature is higher than -3 degrees Celsius. This trend is reasonable: higher temperatures during the melt season accelerate glacier melt, leading to greater mass loss. Therefore, years with higher average temperatures during the melt season typically exhibit negative mass balances, contributing to overall glacier loss in those years.

## 7. Discussion

### *7.1 Differences between In-situ measurements*

In the results section, there are some differences between the in-situ measurements and those obtained using the remote sensing technique. These differences could be attributed to two main reasons. The first reason is the temporal inconsistency between the in-situ and remote sensing measurements. For the remote sensing method, the measurements on all the glaciers are based on data from 2003 to 2023. However, for the in-situ method, the measurements cover a smaller time span.

The second and most important reason for the differences is the variation in glacier boundaries (Table 7). Except for Storglaciären, the in-situ measurements for other glaciers always cover a larger elevation range. The minimum elevations used for in-situ measurements are all lower than those used in the remote sensing method, except for Storglaciären. It is reasonable that all glaciers, except Storglaciären, exhibit a more negative mass balance since regions at lower elevations usually experience more intense glacier melt.

For Storglaciären, the in-situ measurements start from an elevation of 1140 meters, which is 52 meters higher than the lowest elevation considered in the remote sensing method. In higher elevation areas, glaciers lose mass at a much lower rate. This explains why, for Storglaciären, the glacier mass balance measured by the remote sensing method is more negative compared to the in-situ measurements.

Table 7. Area and elevation differences in specific glaciers between remote sensing methods and in-situ measurement

| Study Area | Techniques | Area (km²) | Minimum Elevation (m) | Maximum Elevation (m) |
|---|---|---|---|---|
| Riukojietna (ID:1) | Remote Sensing | 4.09 | 1149 | 1443 |
| | In situ Measurements | 4.65 | 1120 | 1460 |
| Mårmaglaciären (ID:2) | Remote Sensing | 3.70 | 1326 | 1746 |
| | In situ Measurements | 3.96 | 1320 | 1800 |
| Tarfalaglaciären (ID:3) | Remote Sensing | 1.29 | 1387 | 1798 |
| | In situ Measurements | 1.01 | 1380 | 1800 |
| Rabots glaciär (ID:4) | Remote Sensing | 3.45 | 1172 | 1898 |
| | In situ Measurements | 3.95 | 1060 | 1940 |
| Storglaciären (ID:5) | Remote Sensing | 3.69 | 1088 | 1912 |
| | In situ Measurements | 3.21 | 1140 | 1740 |

### *7.2 Representative of Temperature data*

In this master's thesis, only the average temperature during the glacier melt season is analyzed, which is insufficient without including precipitation data. Another problem arises in determining how well the temperature data collected at the research station represents the entire glacier region. In the study area, only the Tarfala station is located among the glaciers in Region A. However, temperature data from Tarfala station cannot represent temperature data for the entire Region A, let alone the whole northern Swedish glacier area.

### *7.3 Non-repeat observation method*

When conducting non-repeat observation methods, the use of a reference DEM is essential. However, incorporating another DEM data introduces additional uncertainty into the results. This uncertainty arises from the inherent errors within the reference DEM data, the altimetry data, and the differences between the two datasets. Furthermore, employing the double difference method to compare elevations across different years compounds these uncertainties.

### *7.4 Time coverage*

For this master's thesis project, available altimetry data spans the years 2003, 2005, 2006, and 2018 to 2023. ICESat-2 provides comprehensive coverage of the entire study area, whereas ICESat data is significantly sparser. To calculate glacier mass changes from 2003 to 2023, using only data from these two years will inevitably increase uncertainties. A better approach would be to generate a complete time series for glacier mass changes, incorporating data from all the intervening years. This method would improve accuracy and reduce uncertainties. Such an approach is feasible for measuring glacier mass differences from 2018 onward using only ICESat-2 altimetry data.

### *7.5 Recommendation for further work*

For future research work in northern Sweden, employing ICESat-2 data presents a promising way due to its extensive coverage across the entire glacier area and its high resolution data. This would facilitate the utilization of near-repeat methods for measuring mass changes, which offer significantly higher accuracy compared to non-repeat methods. With a robust dataset from ICESat-2, researchers may not necessarily require a reference DEM for their investigations, as there would be a sufficient number of near-repeat footprints spanning different years.

Furthermore, researchers employing remote sensing techniques could benefit from gaining insights into the methodologies and practices involved in in-situ measurements, as well as understanding the delineation of glacier boundaries for such measurements. This knowledge exchange would enhance the ability to effectively utilize annual in-situ measurements for evaluating the results obtained from remote sensing methods.

Moreover, addressing the issue of regional climate representativeness is crucial. In future studies, efforts could be made to interpolate temperature data across the entire glacier area, enabling a more comprehensive understanding of climate variability and its impact on glacier dynamics.

## 8. Conclusion

The analysis of glacier mass changes in northern Sweden from 2003 to 2023 employed the non-repeat observation method, utilizing data from ICESat (2003-2009) and ICESat-2 (2018-2023), along with Swedish national DEM, RGI v7.0 glacier boundary, in-situ measurements, and temperature data from the Tarfala station. The total volume decreased by -2.78 ± 0.58 $km^3$, corresponding to a total mass loss of 10.41 ± 6.60 m w.e. over the past two decades. These changes contribute approximately $6.52 \cdot 10^{-3}$ mm to global sea-level rise. The study reveals a general trend of glaciers losing mass throughout the observation period. However, certain years, notably 2005, 2020, and 2022, exhibited an increase in glacier mass compared to the previous year. This fluctuation is influenced by temperature during the melt season, with higher average temperatures leading to more pronounced mass losses in glaciers. Except for Storglaciären, the in-situ measurements of the other glaciers exhibit more negative mass balances compared to those measured by altimetry data. Additionally, as the average temperature of the melt season increases, the glacier mass changes increase.

## References


Allen, S. K., Plattner, G. K., Nauels, A., Xia, Y., & Stocker, T. F. (2014, May). Climate Change 2013: The Physical Science Basis. An overview of the Working Group 1 contribution to the Fifth Assessment Report of the Intergovernmental Panel on Climate Change (IPCC). In EGU General Assembly Conference Abstracts (p. 3544).

Bamber, J. L., & Payne, A. J. (Eds.). (2004). Mass balance of the cryosphere: observations and modelling of contemporary and future changes. Cambridge University Press.

Belart, J. M., Magnússon, E., Berthier, E., Gunnlaugsson, Á. Þ., Pálsson, F., Aðalgeirsdóttir, G., Pálsson, F., Aðalgeirsdóttir, G., Jóhannesson, T., Thorsteinsson, T., & Björnsson, H. (2020). Mass balance of 14 Icelandic glaciers, 1945–2017: spatial variations and inks with climate. Frontiers in Earth Science, 8, 163.

Berthier, E., Schiefer, E., Clarke, G. K., Menounos, B., & Rémy, F. (2010). Contribution of Alaskan glaciers to sea-level rise derived from satellite imagery. Nature Geoscience, 3(2), 92-95.

Berthier, E., Floricioiu, D., Gardner, A. S., Gourmelen, N., Jakob, L., Paul, F., Treichler, D., Wouters, B., Belart, J. M. C., Dehecq, A., Dussaillant, I., Hugonnet, R., Kaab, A. M., Krieger, L., Pálsson, F., & Zemp, M. (2023). Measuring Glacier Mass Changes from pace—A Review. Reports on Progress in Physics, 86(3), 036801.

Bowen, N. (2002). Canary in a coal mine. Climbing News 208(90–97), 138-39.

Brenner, A. C., DiMarzio, J. P., & Zwally, H. J. (2007). Precision and accuracy of satellite radar and laser altimeter data over the continental ice sheets. IEEE Transactions on Geoscience and Remote Sensing, 45(2), 321-331.

Brugger, K. A., Refsnider, K. A., & Whitehill, M. F. (2005). Variation in glacier length and ice volume of Rabots Glaciär, Sweden, in response to climate change, 1910–2003. Annals Glaciology, 42, 180-188.

Davies, B. (2023). Calculating glacier ice volumes and sea level equivalents. AntarcticGlaciers.org.https://www.antarcticglaciers.org/glaciers-and climate/estimating-glacier-contribution-to-sea-level-rise/

Fan, Y., Ke, C. Q., Zhou, X., Shen, X., Yu, X., & Lhakpa, D. (2023). Glacier mass-balance estimates over High Mountain Asia from 2000 to 2021 based on ICESat-2 and NASADEM. Journal of Glaciology, 69(275), 500-512.

Florinsky, I. (2016). Digital terrain analysis in soil science and geology. Academic Press.

Haeberli, W. I. L. F. R. I. E. D. (1995). Glacier fluctuations and climate change detection. Geogr. Fis. Dinam. Quat, 18, 191-199.

Holmlund, P., & Jansson, P. (1999). The Tarfala mass balance programme. Geografiska Annaler: Series A, Physical Geography, 81(4), 621-631.

Hugonnet, R., McNabb, R., Berthier, E., Menounos, B., Nuth, C., Girod, L., Farinotti, D., Huss, M., Dussaillant, I., Brun, F., Kääb, A., (2021). Accelerated global glacier mass loss in the early twenty-first century. Nature 592(7856), 726–731.

Huss, M. (2013). Density assumptions for converting geodetic glacier volume change to mass change. The Cryosphere, 7(3), 877-887.

Jakob, L., Gourmelen, N., Ewart, M., & Plummer, S. (2021). Spatially and temporally resolved ice loss in High Mountain Asia and the Gulf of Alaska observed by CryoSat-2 swath altimetry between 2010 and 2019. The Cryosphere, 15(4), 1845-1862.

Jairo, S. (2016). ICESat. National Aeronautics and Space Administration. https://icesat.gsfc.nasa.gov/icesat/

Jet propulsion laboratory. (2004). ASTER, Advanced Spaceborne Thermal Emission and Reflection Radiometer. Jet propulsion laboratory, California Institute of Technology. https://asterweb.jpl.nasa.gov/

Jim, A. (n.d.). The Human Altimeter Activity. National Aeronautics and Space Administration. https://attic.gsfc.nasa.gov/glas/human.html

Jóhannesson, T., Raymond, C., & Waddington, E. D. (1989). Time–scale for adjustment of glaciers to changes in mass balance. Journal of Glaciology, 35(121), 355-369.

Kääb, A. (2008). Glacier volume changes using ASTER satellite stereo and ICESat GLAS laser altimetry. a test study on Edgeøya, eastern Svalbard. IEEE Trans. Geosci. Remote. Sens., 46(10), 2823-2830.

Kurtis, T. (2024). TERRA, the EOS Flagship. National Aeronautics and Space Administration. https://terra.nasa.gov/about

Lantmäteriet. (2023). Terrain Model Download, grid 50+. Lantmäteriet. https://www.lantmateriet.se/sv/geodata/vara-produkter/produktlista/markhojdmodell-nedladdning-grid-50/

Lemke, P., Ren, J., Alley, R. B., Allison, I., Carrasco, J., Flato, G., Fujii, Y., Kaser, G., Mote, P., & Thomas, R. H. (2007). Observations. Changes in Snow, Ice and Frozen Ground. Chapter 4.

Li, B., Zhu, A. X., Zhang, Y., Pei, T., Qin, C., & Zhou, C. (2006). Glacier change over the past four decades in the middle Chinese Tien Shan. Journal of Glaciology, 52(178), 425-432.

Luthcke, S. B., Thomas, T. C., Pennington, T. A., Rebold, T. W., Nicholas, J. B., Rowlands, D. D., Gardner, A. S., & Bae, S. (2021). ICESat‐2 pointing calibration and geolocation performance. Earth and Space Science, 8(3), e2020EA001494.

Moberg, A. (2011). Tarfala Data. Bolin Centre For Climate Research. https://bolin.su.se/data/tarfala/glaciers.php

Moholdt, G., Nuth, C., Hagen, J. O., & Kohler, J. (2010). Recent elevation changes of Svalbard glaciers derived from ICESat laser altimetry. Remote Sensing of Environment, 114(11), 2756-2767.

National Aeronautics and Space Administration. (n.d.). ASTER Overview. National Aeronautics and Space Administration. https://lpdaac.usgs.gov/data/get-started-data/collection-overview/missions/aster-overview/

National Snow and Ice Data Center. (2023). OpenAltimetry. Earthdata, open access for open science. https://openaltimetry.earthdatacloud.nasa.gov/data/

National Snow and Ice Data Center. (2021). Data Processing Levels. Earthdata, open access for open science. https://www.earthdata.nasa.gov/engage/open-data-services-and-software/data-information-policy/data-levels

National Snow and Ice Data Center. (2024). ICESat/GLAS. National Snow and Ice Data Center, a part of CIRES at the University of Colorado Boulder. https://nsidc.org/data/icesat

National Snow and Ice Data Center. (2024). ICESat-2. National Snow and Ice Data Center, a part of CIRES at the University of Colorado Boulder. https://nsidc.org/data/icesat-2

Neumann, T. A., Martino, A. J., Markus, T., Bae, S., Bock, M. R., Brenner, A. C., Brunt, K. M., Cavanaugh, J., Fernandes, S. T., Hancock, D. W., Harbeck, K., Lee, J., Kurtz, N. T., Luers, P. J., Luthcke, S. B., Magruder, L., Pennington, T. A., Ramos-Izquierdo, L., Rebold, T., Skoog, Jonah., Thomas, T. C. (2019). The Ice, Cloud, and Land Elevation Satellite–2 Mission: A global geolocated photon product derived from the advanced topographic laser altimeter system. Remote sensing of environment, 233, 111325.

Paul, F., Bolch, T., Briggs, K., Kääb, A., McMillan, M., McNabb, R., Nagler, T., Nuth, C., Rastner, P., Strozzi, T., Wuite, J., (2017). Error sources and guidelines for quality assessment of glacier area, elevation change, and velocity products derived from satellite data in the Glaciers_cci project. Remote Sensing of Environment. 203, 256–275.

Paul, F., Bolch, T., Kääb, A., Nagler, T., Nuth, C., Scharrer, K., Shepherd, A., Strozzi, T., Ticconi, F., & Bhambri, R. (2015). The glaciers climate change initiative: Methods for creating glacier area, elevation change and velocity products. Remote Sensing of Environment, 162, 408-426.

Raup, B. H., Kieffer, H. H., Hare, T. M., & Kargel, J. S. (2000). Generation of data acquisition requests for the ASTER satellite instrument for monitoring a globally distributed target: Glaciers. IEEE Transactions on Geoscience and Remote Sensing, 38(2), 1105-1112.

RGI 7.0 Consortium, (2023). Randolph Glacier Inventory - A Dataset of Global Glacier Outlines, Version 7.0. Boulder, Colorado USA. NSIDC: National Snow and Ice Data Center. doi:10.5067/f6jmovy5navz. Online access: https://doi.org/10.5067/f6jmovy5navz

Schutz, B. E., Zwally, H. J., Shuman, C. A., Hancock, D., & DiMarzio, J. P. (2005). Overview of the ICESat mission. Geophysical research letters, 32(21).

Slobbe, D. C., Lindenbergh, R. C., & Ditmar, P. (2008). Estimation of volume change rates of Greenland's ice sheet from ICESat data using overlapping footprints. Remote Sensing of Environment, 112(12), 4204-4213.

SMHI. (2024). Nederbörd. Sveriges meteorologiska och hydrologiska institute. https://www.smhi.se/data/meteorologi/nederbord

Thibert, E., Blanc, R., Vincent, C., & Eckert, N. (2008). Glaciological and volumetric mass-balance measurements: error analysis over 51 years for Glacier de Sarennes, French Alps. Journal of Glaciology, 54(186), 522–532.

Werner, N., Oehler, S., Rendlert, F., & Gunnarson, B. (2024). Reduced accuracy in dendroglaciological mass balance reconstruction of Storglaciären since the 1980s. The Holocene, 34(3), 366-372.

Yi, S., Song, C., Heki, K., Kang, S., Wang, Q., & Chang, L. (2020). Satellite-observed monthly glacier and snow mass changes in southeast Tibet: implication for substantial meltwater contribution to the Brahmaputra. The Cryosphere, 14(7), 2267-2281.

Zhao, F., Long, D., Li, X., Huang, Q., & Han, P. (2022). Rapid glacier mass loss in the Southeastern Tibetan Plateau since the year 2000 from satellite observations. Remote Sensing of Environment, 270, 112853.